# Supporting Information

## Howard et al. 10.1073/pnas.1307784111

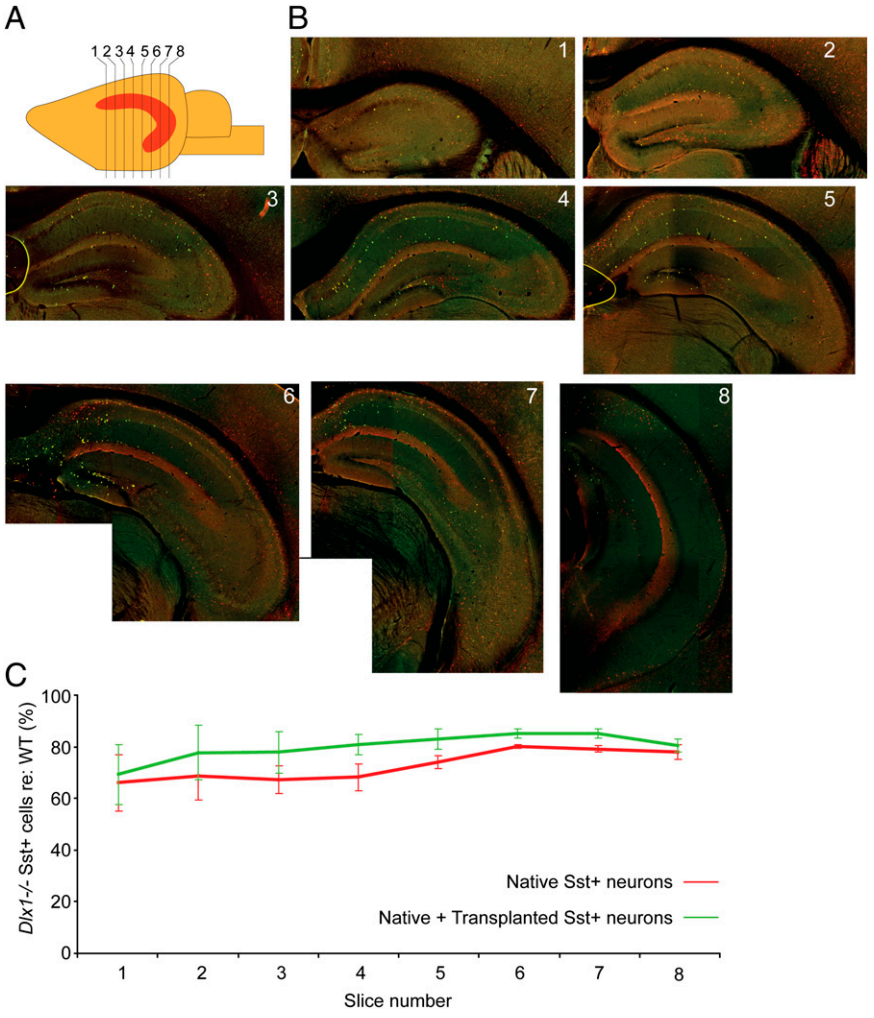


**Fig. S1.** Somatostatin-positive ($Sst^+$) interneuron numbers in the WT, distal-less homeobox 1 ($Dlx1^{-/-}$), and transplanted $Dlx1^{-/-}$ hippocampus. (*A*) Cartoon illustration of the postnatal day (P) 35 hippocampus and the orientation of sections. The numbered black lines indicate example sections through the hippocampus and correlate with the images below. (*B*) Representative coronal sections (50-μm sections separated by 300 μm) through the hippocampus of a P35 $Dlx1^{-/-}$ mouse transplanted at P2. Sections were stained with red fluorescent antibody to Sst and green fluorescent antibody to GFP to label transplanted interneurons. (*C*) Mean native (red) and total (native + transplanted; green) $Sst^+$ interneuron density across sections of $Dlx1^{-/-}$ hippocampi ($n = 3$) normalized to WT $Sst^+$ numbers ($n = 5$).

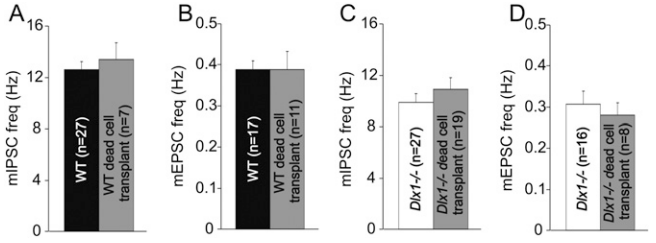


**Fig. S2.** Dead medial ganglionic eminence (MGE) cell transplantation does not alter inhibitory or excitatory synaptic transmission. Dead MGE cell transplantation (DCT) at P2 had no significant effect ($P > 0.05$, *t* tests) on miniature inhibitory postsynaptic current (mIPSC) frequency in WT (*A*; WT = 12.57 ± 0.66 Hz, $n = 27$; WT DCT = 13.34 ± 1.28 Hz, $n = 7$) or $Dlx1^{-/-}$ (*B*; $Dlx1^{-/-}$ = 9.86 ± 0.71 Hz, $n = 27$; $Dlx1^{-/-}$ DCT = 10.89 ± 0.89 Hz, $n = 19$) mice or on miniature excitatory postsynaptic current (mEPSC) frequency in WT (*C*; WT = 0.388 ± 0.023 Hz, $n = 16$; WT DCT = 0.388 ± 0.046 Hz, $n = 11$) or $Dlx1^{-/-}$ (*D*; $Dlx1^{-/-}$ = 0.307 ± 0.030 Hz, $n = 17$; $Dlx1^{-/-}$ DCT = 0.281 ± 0.028 Hz, $n = 8$) mice.

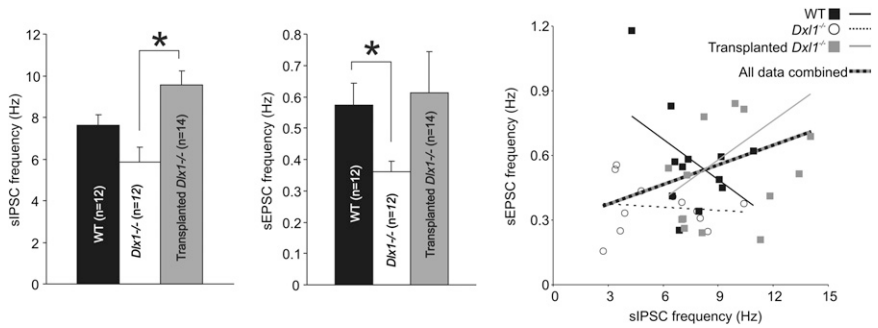


**Fig. S3.** Spontaneous inhibitory and excitatory synaptic event frequencies do not linearly correlate in individual neurons. Spontaneous inhibitory postsynaptic current (sIPSC) frequency (*Left*; WT = 7.62 ± 0.50 Hz, $n = 12$; $Dlx1^{-/-}$ = 5.85 ± 0.72 Hz, $n = 12$; transplanted $Dlx1^{-/-}$ = 9.54 ± 0.69 Hz, $n = 14$; $^*P < 0.001$, one-way ANOVA) and spontaneous excitatory postsynaptic current (sEPSC) frequency (*Center*; WT = 0.572 ± 0.070, $n = 12$; $Dlx1^{-/-}$ = 0.361 ± 0.033 Hz, $n = 12$; transplanted $Dlx1^{-/-}$ = 0.611 ± 0.131 Hz, $n = 14$; $^*P < 0.05$, one-way ANOVA) in WT, $Dlx1^{-/-}$, and MGE-transplanted $Dlx1^{-/-}$ CA1 pyramidal neurons exhibit patterns similar to those shown by mIPSC and mEPSC data. (*Right*) Scatter plots of these two measures made in single neurons show no significant linear correlation between the two measures for any of the three groups ($R^2$ values: WT = 0.21, $Dlx1^{-/-}$ = 0.012, transplanted $Dlx1^{-/-}$ = 0.10).

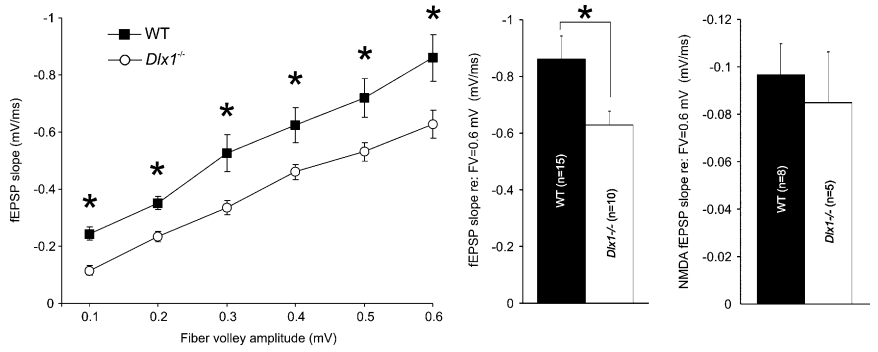


**Fig. S4.** Field potentials reveal decreased AMPA-mediated but normal NMDA-mediated synaptic transmission in $Dlx1^{-/-}$ hippocampus. (*Left*) Input/output function of the field excitatory postsynaptic potential (fEPSP) slope plotted as a function of fiber volley (FV) amplitude reveals decreased synaptic responses in $Dlx1^{-/-}$ slices relative to WT across a broad range of stimulus intensities (FV = 0.1: WT = 0.243 ± 0.023 mV/ms, $n = 20$; $Dlx1^{-/-}$ = 0.115 ± 0.017, $n = 15$; FV = 0.2: WT = 0.352 ± 0.024 mV/ms, $n = 20$; $Dlx1^{-/-}$ = 0.233 ± 0.018, $n = 15$; FV = 0.3: WT = 0.527 ± 0.064 mV/ms, $n = 20$; $Dlx1^{-/-}$ = 0.336 ± 0.025, $n = 15$; FV = 0.4: WT = 0.625 ± 0.061 mV/ms, $n = 20$; $Dlx1^{-/-}$ = 0.46 ± 0.026, $n = 15$; FV = 0.5: WT = 0.721 ± 0.068 mV/ms, $n = 20$; $Dlx1^{-/-}$ = 0.532 ± 0.032, $n = 15$; FV = 0.6: WT = 0.86 ± 0.082 mV/ms, $n = 20$; $Dlx1^{-/-}$ = 0.628 ± 0.051, $n = 15$; $^*P < 0.05$, *t* tests). At high stimulus levels (FV = 0.6 mV), the fEPSP slope was decreased (*Center*) but the isolated NMDA-mediated fEPSP slope was unchanged (*Right*) from WT (WT = 0.097 ± 0.013 mV/ms, $n = 8$; $Dlx1^{-/-}$ = 0.085 ± 0.021, $n = 5$; $^*P > 0.05$, *t* tests).

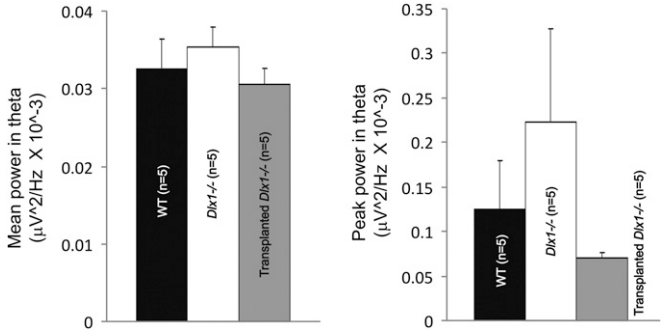


**Fig. S5.** Data for theta oscillations in local field potential recordings. Mean power (*Left*; WT = 0.0306 ± 0.00206, $n = 5$; $Dlx1^{-/-}$ = 0.0353 ± 0.00261, $n = 5$; transplanted $Dlx1^{-/-}$ = 0.0326 ± 0.0085 Hz, $n = 5$; $P > 0.05$, one-way ANOVA) and peak power (*Right*; WT = 0.125 ± 0.054, $n = 5$; $Dlx1^{-/-}$ = 0.223 ± 0.104, $n = 5$; transplanted $Dlx1^{-/-}$ = 0.071 ± 0.0062 Hz, $n = 5$; $P > 0.05$, one-way ANOVA) in the theta frequency band over the same 5-min epoch illustrated in Fig. 6*B*.

**Table S1. Transplanted cells colabeling for neuronal markers**

| Marker | $GFP^+$ cells colabeled ± SEM, % |
|---|---|
| NeuN | 85.2 ± 1.85 |
| GAD67 | 61.2 ± 3.49 |
| Sst | 36.2 ± 4.12 |
| PV | 22.5 ± 2.19 |
| NPY | 3.56 ± 0.50 |
| CR | 6.98 ± 1.16 |
| GFAP | 0.60 ± 0.60 |

$n = 5$ for each marker. CR, calretinin; NeuN, RNA binding protein, fox-1 homolog (*C. elegans*) 3; NPY, neuropeptide Y; PV, parvalbumin; Sst, somatostatin; GAD67, glutamic-acid decarboxylase.

**Table S2. Quantification of inhibitory synaptic transmission in WT, *Dlx1*$^{-/-}$, and transplanted *Dlx1*$^{-/-}$ mice**

| Measure | WT | *Dlx1*$^{-/-}$ | Transplanted *Dlx1*$^{-/-}$ |
|---|---|---|---|
| P21 mIPSC amplitude, pA | 24.06 ± 1.66 (17) | 21.57 ± 1.57 (18) | |
| P21 mIPSC frequency, Hz | 10.52 ± 0.74 (17) | 10.55 ± 0.78 (18) | |
| P35 mIPSC amplitude, pA | 22.36 ± 1.83 (27) | 25.85 ± 2.0 (27) | 25.19 ± 3.1 (11) |

Total population numbers are shown in parentheses. *Dlx1*$^{-/-}$, distal-less homeobox 1; mIPSC, miniature inhibitory postsynaptic current; P, postnatal day.

**Table S3. Quantification of excitatory synaptic transmission in WT, *Dlx1*$^{-/-}$, and transplanted *Dlx1*$^{-/-}$ mice**

| Measure | WT | *Dlx1*$^{-/-}$ | Transplanted *Dlx1*$^{-/-}$ |
|---|---|---|---|
| P21 mEPSC amplitude, pA | 11.90 ± 1.1 (6) | 10.72 ± 0.83 (14) | |
| P21 mEPSC frequency, Hz | 0.275 ± 0.042 (6) | 0.259 ± 0.029 (14) | |
| P35 mEPSC amplitude, pA | 12.65 ± 0.61 (15) | 13.48 ± 0.76 (11) | |
| P35 mEPSC rise time, ms | 1.65 ± 0.16 (5) | 1.59 ± 0.17 (6) | |
| P35 mEPSC decay tau, ms | 9.78 ± 0.61 (15) | 8.94 ± 0.49 (11) | |
| P35 paired pulse ratio | 1.98 ± 0.091 (15) | 1.97 ± 0.088 (20) | 2.05 ± 0.096 (23) |

Total population numbers are shown in parentheses. mEPSC, miniature excitatory postsynaptic current.

**Table S4. Action potential characteristics in response to long-duration current steps**

| Measure | WT ($n = 20$) | Dlx1$^{-/-}$ ($n = 21$) | *P* value |
|---|---|---|---|
| Voltage threshold | −46.87 ± 0.36 mV | −46.35 ± 0.65 mV | 0.49 |
| Action potential amplitude | 101.06 ± 1.47 mV | 101.69 ± 2.43 mV | 0.91 |
| Action potential half-width | 1.23 ± 0.041 ms | 0.995 ± 0.032 ms | <0.001* |
| No. of action potentials to 500-pA current step | 31.15 ± 2.62 | 24.86 ± 1.59 | 0.04* |

*P* values are taken from paired *t* tests. Total population numbers are shown in parentheses.
*Significant *P* value.

**Table S5. Quantification of gamma frequency oscillations in WT, *Dlx1*$^{-/-}$, and transplanted *Dlx1*$^{-/-}$ mice**

| Measure | WT | *Dlx1*$^{-/-}$ | Transplanted *Dlx1*$^{-/-}$ |
|---|---|---|---|
| Mean theta power | 0.0326 ± 0.0038 | 0.0353 ± 0.00261 | 0.0306 ± 0.00206 |
| Peak theta power | 0.125 ± 0.0539 | 0.223 ± 0.104 | 0.0705 ± 0.0062 |
| Mean gamma power | $4.0 * 10^{-3} \pm 0.20 * 10^{-3}$ | $4.93 * 10^{-3} \pm 0.30 * 10^{-3}$ | $4.38 * 10^{-3} \pm 0.27 * 10^{-3}$ |

Units are expressed as squared microvolts per hertz. $n = 5$ for each group.